NEUROPATHOLOGY

Neuropathology 2014; **34**, 190–196 doi:10.1111/neup.12076

Case Report

Globoid cell leukodystrophy (Krabbe's disease) in a Japanese domestic cat

Mizue Ogawa,[1] Kazuyuki Uchida,[1] Kyoko Isobe,[3] Miyoko Saito,[2] Tomoyuki Harada,[1] James K. Chambers[1] and Hiroyuki Nakayama[1]

[1]Department of Veterinary Pathology, Graduate School of Agricultural and Life Sciences, The University of Tokyo, Tokyo, Departments of [2]Surgery II and [3]Veterinary Teaching Hospital, School of Veterinary Medicine, Azabu University, Kanagawa, Japan

A male Japanese domestic cat developed progressive limb paralysis from 4 months of age. The cat showed visual disorder, trismus and cognitive impairment and died at 9 months of age. At necropsy, significant discoloration of the white matter was observed throughout the brain and spinal cord. Histologically, severe myelin loss and gliosis were observed, especially in the internal capsule and cerebellum. In the lesions, severe infiltration of macrophages with broad cytoplasm filled with PAS-positive and non-metachromatic granules (globoid cells) was evident. On the basis of these findings, the case was diagnosed as feline globoid cell leukodystrophy (Krabbe's disease). Immunohistochemical observation indicated the involvement of oxidative stress and small HSP in the disease.

Key words: cat, central nervous system, globoid cell leukodystrophy, Krabbe's disease, macrophages.

INTRODUCTION

Globoid cell leukodystrophy (GLD; also known as Krabbe's disease) is an early-onset, rapidly progressive and fatal degenerative disease. The disease is pathologically characterized by almost complete myelin loss, reactive astrocytosis and the appearance of characteristic large round cells called globoid cells in the white matter of the CNS.[1] Diseases identical to GLD have been reported in several animal species:[2] dogs,[3,4] sheep,[5] rhesus monkeys[6,7] and cats.[8–10] GLD is defined by the deficiency of a lysosomal enzyme, galactocerebrosidase (GALC), resulting in the accumulation of a cytotoxic metabolite, psychosine.[1] GALC-deficient mice, such as Twitcher mice,[11,12] are being used as experimental GLD models.[13] Besides GALC, the deficiency of saposin A, [14] one of the sphingolipid activator proteins, also causes an identical disease to GLD in mice[15] and humans.[10] While GALC mutation was found in dogs[16] and rhesus monkeys.[17] To date, there have been only three reports of the disease in cats,[8–10] indicating that the disease is extremely rare in cats. These previous reports on feline GLD revealed histopathological features characterized by symmetrical myelin loss, astrocytosis and perivascular accumulation of large macrophages with intracytoplasmic deposits (globoid cells).

The present report describes histopathological, immunohistochemical and ultrastructural features of GLD in a young cat. In addition, immunohistochemistry for nitric oxide (NOS) and two types of small HSP (sHSP) was performed to assess the involvement of oxidative stress and/or sHSP, which are commonly upregulated in glial cells in patients with neurodegenerative diseases.[18]

CLINICAL SUMMARY

A male Japanese domestic cat had exhibited hind limb paresis since 4 months of age. Then the symptom progressed and clear tetraparesis developed. Although temporary recovery was achieved, loss of voluntary movement, trismus, and visual and cognitive impairment were observed during the last 2 months before death at 9 months of age. No significant findings were detected by X-ray examination or hematologic and biochemical analyses. The serum antibodies for feline immunodeficiency virus (FIV), feline leukemia virus (FeLV), feline coronavirus, feline parvovirus and *Toxoplasma* were all negative.

Correspondence: Kazuyuki Uchida, DVM, PhD, Department of Veterinary Pathology, Graduate School of Agricultural and Life Sciences, The University of Tokyo, 1-1-1 Yayoi, Bunkyo-ku, Tokyo 113-8657, Japan. Email: auchidak@mail.ecc.u-tokyo.ac.jp

Received 7 August 2013; revised 29 August 2013 and accepted 24 September 2013; published online 8 November 2013.

MATERIALS AND METHODS

Tissue samples including the brain, spinal cord and brachial plexus were fixed in 10% neutral-buffered formalin, processed routinely and embedded in paraffin wax. Paraffin sections 4 μm thick were stained with HE. Some selected sections were also subjected to PAS, toluidine blue (TB, pH 7.0), LFB, Sudan-black and von-Kossa staining. Immunohistochemistry was performed using the Envision polymer method. The primary antibodies used are listed in Table 1. Deparaffinized sections were first autoclaved at 120°C for 10 min in 10 mmol/L citrate buffer (pH 6.0) or Target retrieval solution (pH 9.0), for antigen retrieval. Then, the tissue sections were treated with 3% hydrogen peroxide (H_2O_2)-methanol at room temperature for 5 min and incubated in 8% skimmed milk–Tris-buffered saline with 0.2% Tween 20 (TBST) at 37°C for 1 h to avoid nonspecific reactions. The sections were then incubated at 4°C overnight with one of the primary antibodies. After washing three times in TBST, the sections were incubated with Envision horseradish peroxidase (HRP) mouse or rabbit polymer (Dako, Glostrup, Denmark) at 37°C for 40 min Then, the sections were washed with TBS and visualized with 0.05% 3-3'diaminobenzidine and 0.03% H_2O_2 in TBS. Counterstaining was performed with Mayer's hematoxylin.

For electron microscopic analysis, the formalin-fixed cerebellar white matter was fixed again in 2% glutaraldehyde in 0.1 mol/L phosphate buffer (PB) at 4°C for 2 h, and post-fixed in 1% OsO_4 at 4°C for 2 h. The samples were dehydrated in an ethanol series, replaced with QY-1 solution (Nisshin EM Corporation, Tokyo, Japan) and embedded in Quetol651 resin (Nisshin EM). Ultrathin sections were stained with uranyl acetate and lead citrate and examined with a Hitachi H-7500 transmission electron microscope (Hitachi High-Technologies, Tokyo, Japan).

PATHOLOGICAL FINDINGS

No marked gross lesions were detected in the CNS at necropsy, although discoloration of the white matter was observed on the cut surface of the formalin-fixed brain (Fig. 1) and spinal cord.

Histologically, thinning of the white matter was observed throughout the brain and spinal cord. LFB staining (Figs 2,3a) and immunostaining for myelin basic protein (MBP) revealed marked myelin loss in the white matter. Severe axonal degeneration characterized by swollen and fragmented axons (Fig. 3b) was also observed. Astrocytosis (Fig. 3c) and infiltration of ionized calcium-binding adapter molecule 1 (Iba-1)-positive cells (Fig. 3d) were frequently observed in the lesions. Oligodendrocyte transcription factor 2 (Olig2)-positive oligodendrocytes slightly decreased in number. These lesions were severe in the white matter of the internal capsule, cerebellum, medulla and spinal cord, but relatively less severe in the white matter of the cerebrum. In the deep white matter of the cerebellum, focal and symmetric necrosis was evident. In the necrotic areas, there were many calcified deposits forming psammoma bodies. The bodies were stained with LFB, PAS and von Kossa (Fig. 4).

Table 1 Primary antibodies used

Antibody	Type	Dilution	Source	Marker for	Antigen retrieval
GFAP	p	1:1000	Dako, Glostrup, Denmark	Astrocyte	None
NF	m	pre-diluted	Dako	Axon/neuron	None
pNF-H&M	m	1:1000	Millipore, MA, USA	–	None
MBP	p	1:200	Dako	Myelin	Citrate buffer, pH 6.0
Olig2	p	1:500	Millipore	Oligodendrocyte	Target retrieval solution (Dako), pH 9.0
CD3	p	1:50	Dako	T cell	Citrate buffer, pH 6.0
CD20	p	1:200	Thermo Scientific, CA, USA	B cell	None
Iba1	p	1:500	Wako Pure Chemical Industries, Osaka, Japan	Microglia/macrophage	Citrate buffer, pH 6.0
HLA-DR	m	1:100	Dako	Macrophage	Citrate buffer, pH 6.0
HSP27	p	1:100	Cell Signaling Technology, MA, USA	–	Citrate buffer, pH 6.0
αB-crystallin	m	1:1000	Santa Cruz Biotechnology, CA, USA	–	Citrate buffer, pH 6.0
iNOS	p	1:200	Calbiochem, CA, USA	–	Citrate buffer, pH 6.0
HO-1	p	1:100	ENZO Life Sciences, Plymouth Meeting, PA, USA	–	Citrate buffer, pH 6.0
SOD1	p	1:200	ENZO Life Sciences	–	Citrate buffer, pH 6.0
SOD2	p	1:200	ENZO Life Sciences	–	Citrate buffer, pH 6.0

HLA-DR, humanleukocyte antigen type DR; HO-1, heme oxygenase-1; Iba1, ionized calcium-binding adapter molecule 1; iNOS, inducible nitric oxide synthase; m, mouse monoclonal; MBP, myelin basic protein; NF, neurofilament; Olig2, oligodendrocyte transcription factor 2; p, rabbit polyclonal; SOD, superoxide dismutase.

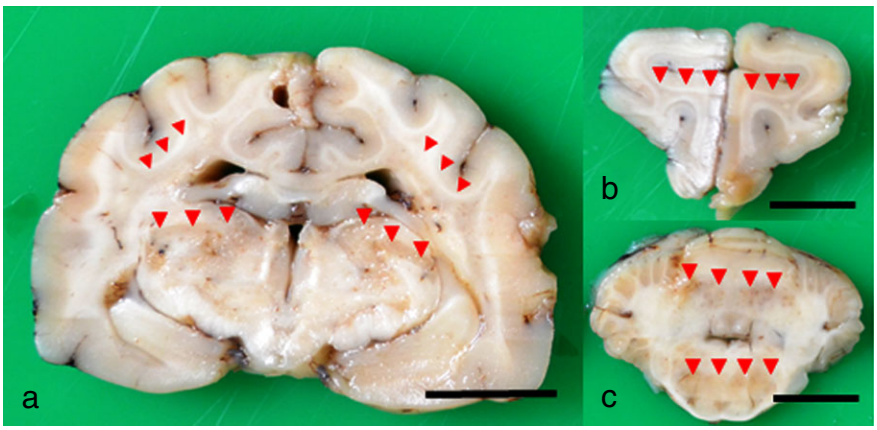

Fig. 1 Cut surfaces of the formalin-fixed brain. Severe discoloration throughout the white matter (arrowheads). (a) Cerebrum and thalamus, hypothalamus level. (b) Frontal lobe. (c) Cerebellum and ventral pons. Scale bar = 1 cm.

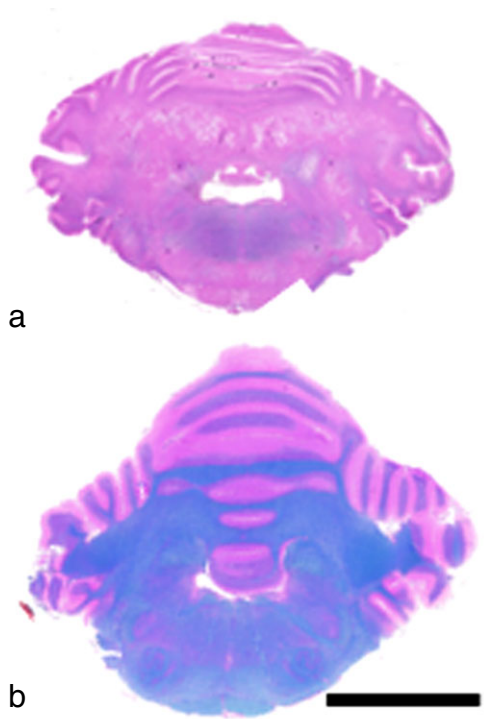

Fig. 2 The cerebellum. LFB-HE. (a) The present case. (b) A normal adult cat. Almost complete myelin loss is observed in the present case (a), compared with the control (b). Scale bar = 1 cm.

In the gray matter throughout the brain and spinal cord, prominent proliferation of gemistocytic astrocytes was observed. In the cerebellar cortex, there was moderate loss of granule cells and Purkinje cells with proliferation of Bergmann's glia. Neurofilament- and phosphorylated neurofilament-positive torpedoes were frequently observed in the granular cell layer (Fig. 5).

A large number of macrophages with broad cytoplasm and single or multiple eccentric nuclei (globoid cells) were observed in the lesions of the brain white matter, especially in the perivascular area (Fig. 6a). In the thoracic and lumbar cord, where myelin and axons were completely lost, there were a few globoid cells. Immunohistochemically, these globoid cells were strongly positive for Iba-1 (Fig. 6a, insertion) and HLA type DR (HLA-DR). The globoid cells had fine granular or filamentous deposits in their cytoplasm, which were PAS-positive (Fig. 6b), Sudan-black-negative and non-metachromatic by TB staining (Fig. 6c). Ultrastructural examination indicated the detailed features of the cytoplasmic deposits: variably sized, and straight and curved tubular structures (Fig. 6d). In the same area, mild perivascular infiltration of CD3-positive lymphocytes was also observed, whereas there was no infiltration of CD20-positive cells.

The results of immunohistochemistry also demonstrated that the cytoplasm of the globoid cells and of the few reactive astrocytes was positive for inducible nitric oxide (iNOS) (Fig. 7). Superoxide dismutase (SOD)1 expression was seen in reactive astrocytes and degenerated axons. Granules strongly positive for SOD2 were observed in cytoplasm of globoid cells, excluded by cytoplasmic deposit. Reactive astrocytes were occasionally positive for heme oxygenase-1 (HO-1).

On the other hand, reactive astrocytes were mostly positive for αB-crystallin in a broad area of the CNS. HSP27-positive astrocytes were rarely observed.

In the peripheral nerves including the brachial plexus, trigeminal nerve and dorsal and ventral roots of the spinal cord, various levels of myelin loss and axonal degeneration were observed, while there were no globoid cells in the lesions. No significant lesions were observed in the visceral organs.

DISCUSSION

Considering the severe myelin loss throughout the CNS and the appearance of characteristic globoid cells with intracellular PAS-positive and non-metachromatic deposits, the present case was diagnosed as feline GLD. In

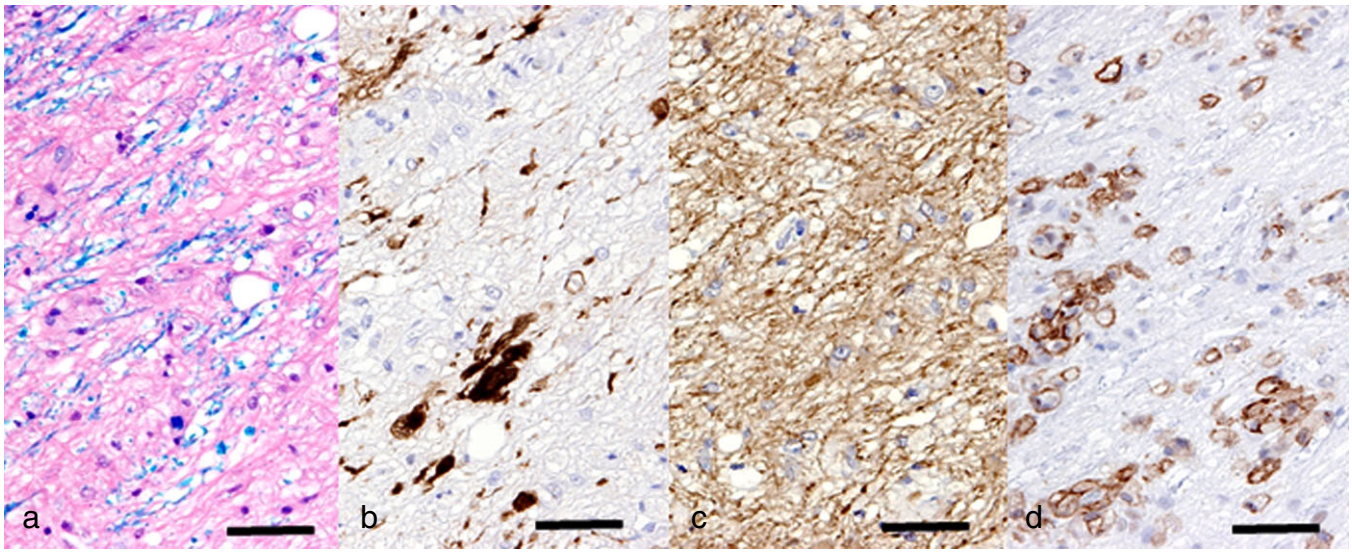

Fig. 3 A lesion of the cerebellar white matter. (a) LFB-HE. Immunostain for (b) neurofilament, (c) GFAP and (d) Iba-1. In addition to myelin loss (a), severe axonal degeneration/loss (b) and astrogliosis (c) are observed in the area with macrophage infiltration (d). Scale bar = 50 μm.

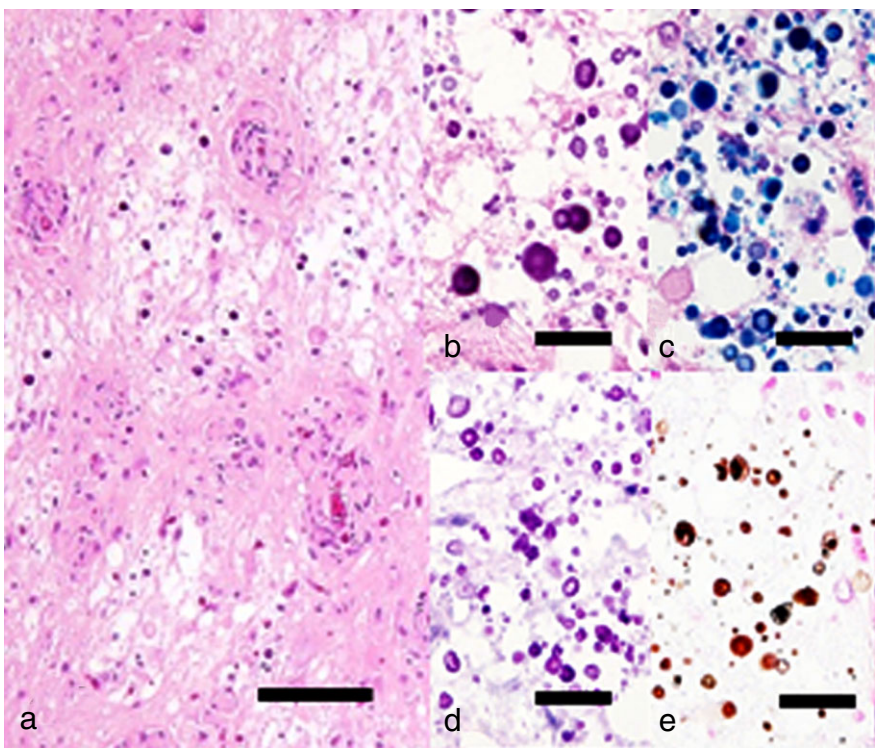

Fig. 4 Psammoma body in the cerebellar white matter. (b)–(e) are higher magnifications of (a): (a) and (b) HE, (c) LFB-HE, (d) PAS, and (e) von Kossa. The eosinophilic deposits were positive for LFB, PAS and von Kossa stains. Scale bar = 100 μm (a) and 25 μm (b–e).

addition, the formation of torpedoes observed in the present case is also common in human GLD.[19]

As far as we know, there have been three reports on spontaneous GLD in cats[8–10] and the distribution of the lesions and histological findings in the present case resemble those of GLD in humans[20] and in cats,[9] indicating that the present feline case is included in the same disease category. This is the first report of GLD in a Japanese domestic cat. In addition, despite the exact age of the cat being unknown, the present case may be relatively old compared with the previous feline GLD cases, probably because of effective care.

Psammoma body-like calcium deposits probably contained decayed products of myelin because they

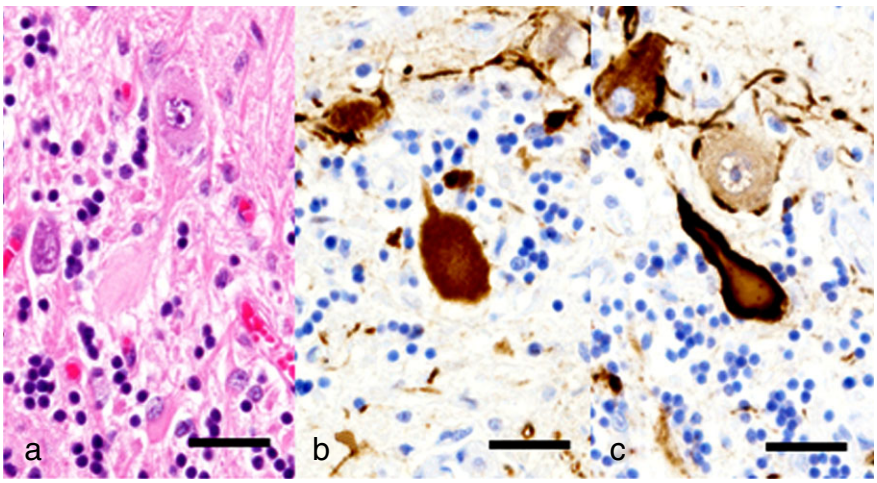

Fig. 5 A torpedo in the cerebellum. (a) HE. Immunostain for (b) neurofilament and (c) phosphorylated neurofilament. Neurofilament- and phospho-neurofilament-positive torpedoes were frequently observed. Scale bar = 25 µm.

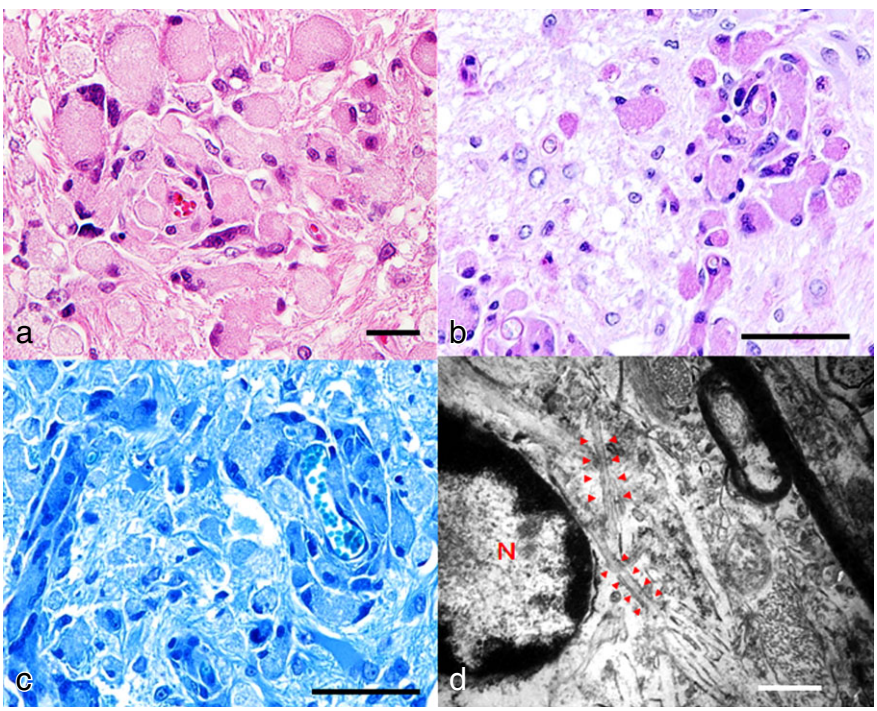

Fig. 6 Globoid cells in the cerebellar white matter. (a) HE, (b) PAS, (c) toluidine blue (TB) and (d) ultrastructural observation of a globoid cell. Globoid cells were round-shaped macrophages with broad cytoplasm (a). The deposits in the cytoplasm of a globoid cell were PAS-positive (b) and non-metachromatic with TB stain (c). Ultrastructurally, fine tubular structures with a diameter of 30–100 nm were accumulated in the cytoplasm of a globoid cell (d). Scale bar = 25 µm (a), 50 µm (b, c) and 500 nm (d).

were LFB-positive. A slight decrease of olig2-positive oligodendrocytes in spite of the severe myelin loss suggests that feline GLD may be a disease mostly caused by the dysfunction of myelination, maybe due to psychosine accumulation, rather than by the degeneration of mature myelin. Biochemical analysis or analysis of GALC or the saposin A gene was not performed because all tissues were unfortunately formalin-fixed at nectropsy because of the suspicion of infectious diseases. To determine whether this feline disease is exactly the same as human GLD, gene analysis should be performed.

The infiltration of CD3-positive T cells into the lesions in the present case indicates the involvement of immunological responses in the pathogenicity of the feline disease, like in human GLD.[19] However, the infiltration was not very severe in view of the longer survival and/or because of steroid treatment.

The production of reactive oxygen species (ROS) was observed in Twitcher mice, a GLD model, as a secondary event following psychosine toxicity.[21] The expression of iNOS, which results in ROS production, was reported to be distributed mostly in GFAP-positive astrocytes in human GLD,[21] and in both astrocytes and globoid cells of GLD of rhesus macaques,[7] as well as in the present case. On the other hand, in the present case, SOD2, a mitochondrial antioxidant enzyme, was strongly expressed by globoid cells themselves. SOD1[17] and HO-1,[23] the molecules usually induced by ROS, were also expressed by reactive

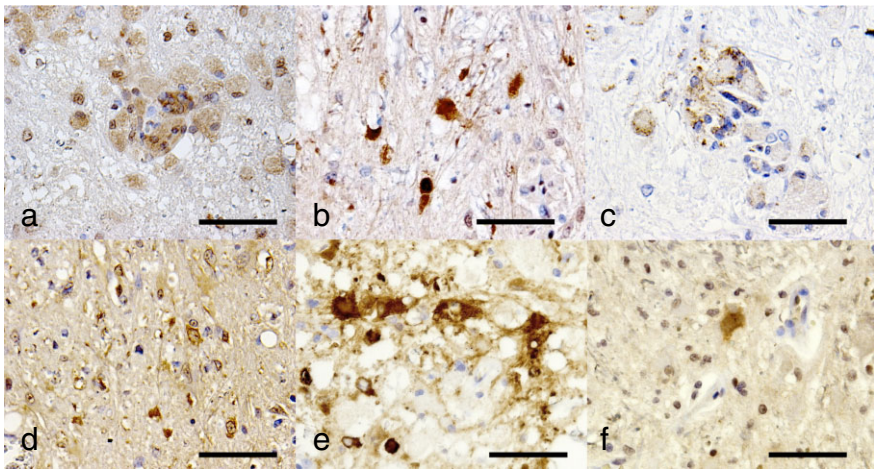

Fig. 7 The cerebellum. Immunohistochemistry for inducible nitric oxide (iNOS), SOD, heme oxygenase-1 (HO-1) and sHSPs. (a) iNOS, (b) SOD1, (c) SOD2, (d) HO-1, (e) αB-crystallin and (f) HSP27. Positive staining for iNOS and SOD2 was observed in the cytoplasm of globoid cells, not including filamentous deposit (a, c). SOD1 (b) and HO-1 (d) expression was occasionally observed in reactive astrocytes. αB-crystallin expression was observed in reactive astrocytes (e), whereas only few astrocytes were positive for HSP27 (f). Scale bar = 50 μm.

astrocytes. Although it is interesting that the iNOS expression patterns vary among animals, it may be a common accelerating factor for disease progression, not an exclusive factor for the pathogenesis. The induction of the antioxidant enzymes may be a physiological consequence in the recovery of neuronal tissue following oxidative damage.

Increased expressions of αB-crystallin and HSP27 were reported in Rosenthal fibers of Alexander's disease and in GFAP-positive gliosis lesions of human neurodegenerative diseases,[18] but the roles of these molecules in the pathogenicity of such neurodegenerative diseases are still controversial. The strong expressions of the molecules in the CNS of the present case suggest involvement of the molecules in disease progression also in feline GLD.

REFERENCES

1. Suzuki K. Globoid cell leukodystrophy (Krabbe's disease): update. *J Child Neurol* 2003; **18** (9): 595–603.
2. Wenger DA. Murine, canine and non-human primate models of Krabbe disease. *Mol Med Today* 2000; **6** (11): 449–451.
3. Fletcher JL, Williamson P, Horan D, Taylor RM. Clinical signs and neuropathologic abnormalities in working Australian Kelpies with globoid cell leukodystrophy (Krabbe disease). *J Am Vet Med Assoc* 2010; **237** (6): 682–688.
4. McGraw RA, Carmichael KP. Molecular basis of globoid cell leukodystrophy in Irish setters. *Vet J* 2006; **171** (2): 370–372.
5. Pritchard DH, Napthine DV, Sinclair AJ. Globoid cell leucodystrophy in polled Dorset sheep. *Vet Pathol* 1980; **17** (4): 399–405.
6. Baskin GB, Ratterree M, Davison BB *et al.* Genetic galactocerebrosidase deficiency (globoid cell leukodystrophy, Krabbe's disease) in rhesus monkeys (Macaca mulatta). *Lab Anim Sci* 1998; **48** (5): 476–482.
7. Borda JT, Alvarez X, Mohan M *et al.* Clinical and immunopathologic alterations in rhesus macaques affected with globoid cell leukodystrophy. *Am J Pathol* 2008; **172** (1): 98–111.
8. Johnson K. Globoid leukodystrophy in the cat. *J Am Vet Med Assoc* 1970; **157**: 2057–2064.
9. Salvadori C, Modenato M, Corlazzoli D, Arispici M, Cantile C. Clinicopathological features of globoid cell leucodystrophy in cats. *J Comp Pathol* 2005; **132** (4): 350–356.
10. Sigurdson CJ, Basaraba RJ, Mazzaferro EM, Gould DH. Globoid cell-like leukodystrophy in a domestic longhaired cat. *Vet Pathol* 2002; **39** (4): 494–496.
11. Lee WC, Tsoi YK, Dickey CA, DeLucia MW, Dickson DW, Eckman CB. Suppression of galactosylceramidase (GALC) expression in the twitcher mouse model of globoid cell leukodystrophy (GLD) is caused by nonsense-mediated mRNA decay (NMD). *Neurobiol Dis* 2006; **23** (2): 273–280.
12. Sakai N, Inui K, Tatsumi N, Fukushima H *et al.* Molecular cloning and expression of cDNA for murine galactocerebrosidase and mutation analysis of the twitcher mouse, a model of Krabbe's disease. *J Neurochem* 1996; **66** (3): 1118–1124.
13. Potter GB, Santos M, Davisson MT *et al.* Missense mutation in mouse GALC mimics human gene defect and offers new insights into Krabbe disease. *Hum Mol Genet* 2013; **22** (17): 3397–3414.
14. Spiegel R, Bach G, Sury V *et al.* A mutation in the saposin A coding region of the prosaposin gene in an infant presenting as Krabbe disease: first report of saposin A deficiency in humans. *Mol Genet Metab* 2005; **84** (2): 160–166.

15. Matsuda J, Vanier MT, Saito Y, Tohyama J, Suzuki K, Suzuki K. A mutation in the saposin A domain of the sphingolipid activator protein (prosaposin) gene results in a late-onset, chronic form of globoid cell leukodystrophy in the mouse. *Hum Mol Genet* 2001; **10** (11): 1191–1199.
16. Victoria T, Rafi MA, Wenger DA. Cloning of the canine GALC cDNA and idntification of the mutation causing globoid cell leukodystrophy in West Highland White and Cairn terriers. *Genomics* 1996; **33** (3): 457–462.
17. Andersen JK. Oxidative stress in neurodegeneration: cause or consequence? *Nat Med* 2004; **10**: S18–S25.
18. Van Rijk A, Bloemendal H. Alpha-B-crystallin in neuropathology. *Ophthalmologica* 2000; **214** (1): 7–12.
19. Itoh M, Hayashi M, Fujioka Y, Nagashima K, Morimatsu Y, Matsuyama H. Immunohistological study of globoid cell leukodystrophy. *Brain Dev* 2002; **24** (5): 284–290.
20. Percy AK, Odrezin GT, Knowles PD, Rouah E, Armstrong DD. Globoid cell leukodystrophy: comparison of neuropathology with magnetic resonance imaging. *Acta Neuropathol* 1994; **88** (1): 26–32.
21. Hawkins-Salsbury JA, Qin EY, Reddy AS, Vogler CA, Sands MS. Oxidative stress as a therapeutic target in globoid cell leukodystrophy. *Exp Neurol* 2012; **237** (2): 444–452.
22. Giri S, Jatana M, Rattan R, Won JES, Singh I, Singh AK. Galactosylsphingosine (psychosine)-induced expression of cytokine-mediated inducible nitric oxide synthases via AP-1 and C/EBP: implications for Krabbe disease. *FASEB J* 2002; **16** (7): 661–672.
23. Schipper HM, Song W, Zukor H *et al*. Heme oxygenase-1 and neurodegeneration: expanding frontiers of engagement. *J Neurochem* 2009; **110** (2): 469–485.